Acta Cryst. (1974). B30, 1381

Structure Refinement and Random Error Analysis for Strontium 'Chlorapatite', $Sr_5(PO_4)_3Cl$

BY K. SUDARSANAN AND R. A. YOUNG

Georgia Institute of Technology, Atlanta, Georgia 30332, *U.S.A.*

(*Received* 10 *September* 1973; *accepted* 26 *December* 1973)

The crystal is hexagonal, $P6_3/m$, with $a=9{\cdot}859$ (1) and $c=7{\cdot}206$ (2) Å. Least-squares refinements (1174 independent diffractometer-measured reflections, 42 parameters, Mo $K\alpha$ radiation, corrections for absorption and extinction, simultaneous diffraction effects minimized) led to $R(|F|)=0{\cdot}034$ and $wR(|F|)^2=0{\cdot}044$. The general structural features are the same as those of fluorapatite and hydroxyapatite except for the position of the chlorine atom, which is at $0,0,\frac{1}{2}$, midway between the two Sr triangles on the mirror planes at $z=\frac{1}{4}$ and $z=\frac{3}{4}$. Error analysis carried out with normal probability plots and correlation-testing plots showed that over and above the counting statistical errors and instrument instability there was an additional random error, of the order of 5% of $|F|^2$, of unknown origin. Also encountered with other specimens, and thought not to be due to crystal dimension and absorption coefficient errors, this additional error might be due to crystal inhomogeneity with respect to diffraction.

Introduction

Strontium 'chlorapatite' is one of the members of the apatite group having the same basic structure and composition $A_5(MO_4)_3X$, where A is alkali metals, alkaline earths, rare earths, Cd, Pb, Mn, *etc.*; M is P, As, V, Si *etc.*, and X is a halogen or hydroxyl group. While 'fluorapatite', $Ca_5(PO_4)_3F$ (Naray-Szabo, 1930; Sudarsanan, Mackie & Young, 1972), crystallizes in the hexagonal system with space group $P6_3/m$, stoichiometric 'chlorapatite' crystallizes in a very closely related, strongly pseudo-hexagonal, monoclinic structure ($b=2a$, $\gamma=120°$) in space group $P2_1/b$ with chlorine at the site (0,0,0·444) (Mackie, Elliott & Young, 1972). [Usually occurring in $P6_3/m$, $Ca_5(PO_4)_3OH$ also crystallizes in $P2_1/b$ on occasion (Elliott, Mackie & Young, 1973).] In contrast, in $Cd_5(PO_4)_3Cl$, the chlorine occurs at $0,0,\frac{1}{4}$ (Sudarsanan, Young & Donnay, 1972), making it isostructural with fluorapatite.

The strontium analogs of hydroxyapatite (and chlorapatite) hold biological interest because of the ready entry of Sr into the food chain and its subsequent incorporation in bone. The strontium analogs differ somewhat from the calcium apatites in their crystallization characteristics under the same conditions. Strontium present in trace amounts in human tooth enamel, presumably substituted for Ca in the model compound $Ca_5(PO_4)_3OH$, has been suggested to inhibit caries formation (Curzon, Adkins, Bibby & Losee, 1970). It would seem that such differences should find their origins in the structural details of the crystals. The structure of strontium hydroxide phosphate 'strontium hydroxyapatite' has been reported in detail (Sudarsanan & Young, 1972); it is essentially the same as that of hydroxyapatite (Sudarsanan & Young, 1969). The detailed refinement of the strontium 'chlorapatite' structure was undertaken and the particular emphasis then placed on error analysis produced some unexpected results.

Experimental

Crystal growth

Single crystals of strontium chlorapatite were prepared by standard flux growth techniques with excess strontium chloride used as the flux. Strontium hydroxyapatite was first prepared by adding $(NH_4)_2HPO_4$ solution to a solution of $Sr(NO_3)_2$ maintained at 95°C, both solutions being made basic with ethylenediamine (Collin, 1959). A mixture of 80 wt.% of $SrCl_2$ (m.p. 873°C) and 20 wt.% of $Sr_5(PO_4)_3OH$ was then placed in a tightly covered platinum crucible and heated to a temperature of 1280°C in a resistance furnace. After the melt had been kept at this temperature for 24 h, the furnace was cooled at the rate of ~20°C per day to 1080°C and then shut off. The resulting crystals were separated from the melt by repeated washing in distilled hot water and were then filtered out and dried. Clear needle-shaped crystals, of length ~0·06 cm and with hexagonal cross-sections of side about 0·01 cm, were obtained. The particular specimen used for X-ray study was 0·052 mm long with 0·015 mm and 0·013 mm, respectively, maximum and minimum distances between opposing faces. Crystal optical data are: uniaxial positive, length slow, $n_e=1{\cdot}667$, $n_\omega=1{\cdot}664$ for $\lambda=5893$ Å. Chemical analyses of a portion of the batch from which the specimen was taken were reported as 59·07, 36·32, and 4·50 wt.%, respectively, for Sr, PO_4, and Cl. The stoichiometric values are 57·77, 37·56 and 4·67 wt.%, respectively.

Diffraction data

The lattice parameters were determined from least-squares refinements with crystal-setting data for 12 reflections (within the angular range $70°<2\theta<105°$) measured on a computer-controlled four-circle diffractometer with Mo $K\alpha$ radiation, $\lambda=0{\cdot}70926$ Å. A balanced-filter (Zr&Y) ω-scan technique was used for measurement of the intensities of the lower-angle re-

flections for which the absorption edge of Zr fell within the scanning range for peak plus background; the 2θ-scan technique with a Zr filter was used for other reflections ($2\theta < 80°$ for all). Simultaneous diffraction effects were assessed by remeasurement of each reflection intensity after the specimen was rotated about the diffraction vector by one degree. Those measured reflection intensities which, for the two settings of the crystal, differed by more than three times the expected standard deviation (on the basis of counting statistics) were eliminated from further consideration. Each reflection was scanned repeatedly, as required to yield 2% statistical precision (counting statistics) in the net intensities, up to a maximum of 16 times. (Approximately 58% of the 1178 reflections used were measured with a precision of 2% while the other 42% were limited in precision to a roughly estimated average of ~6%.) Absorption corrections were applied by the method of Busing & Levy (1957) with $\mu_l = 235{\cdot}1$ cm^{-1} for Mo $K\alpha$ radiation. The calculated transmission coefficient ranged from 0·065 to 0·115.

Refinement of the structure

A version of the Busing, Martin & Levy (1962) least-squares refinement program as modified by Ellison, Hamilton, Ibers, Johnson & Thiessen (1971), to include anomalous dispersion and isotropic and anisotropic extinction corrections, and called *ORXFLS*3 was used. The sources of atomic scattering factors used were Cromer & Waber (1965) for Sr^{2+}, P and Cl^- and Tokonami (1965) for O^{2-}. Anomalous dispersion corrections were made with values of $\Delta f'$ and $\Delta f''$ calculated by Cromer (1965). The observed structure factors were corrected for isotropic secondary extinction. The final extinction parameter was 0·075. In the refinements, the chlorine atom moved close to $(0,0,\frac{1}{2})$ and was fixed there for several cycles. In the late stages of refinement, a trial refinement of all other variable parameters with Cl fixed at (0,0,0·47) rather than $(0,0,\frac{1}{2})$ led to $wR_2 = 0{\cdot}086$ rather than 0·044. The position $(0,0,\frac{1}{2})$ was therefore accepted as correct and was used in further refinements. The final values of the reliability values are $R_1 = 0{\cdot}034$, $R_2 = 0{\cdot}038$ and $wR_2 = 0{\cdot}044$, where

$$R_1 = \sum (||F_o| - |F_c||) / \sum |F_o|,$$
$$R_2 = \sum (||F_o|^2 - |F_c|^2|) / \sum |F_o|^2$$

and

$$wR_2 = \{ \sum w(|F_o|^2 - |F_c|^2)^2 / \sum w|F_o|^4 \}^{1/2}$$

where w is the reciprocal of the variance estimated from counting statistics.

Results and discussion

The positional and temperature parameters are listed in Table 1 and the bond angles and interatomic distances in Table 2. Structure factors are given in Table 3. $Sr_5(PO_4)_3Cl$ would be isostructural with $Sr_5(PO_4)_3OH$ (Sudarsanan & Young, 1972) except for the chlorine position midway between the two Sr(2) triangles (related to each other by the screw axis) at $z = \frac{1}{4}$ and

Table 2. *Bond angles and interatomic distances*† (*standard deviation, in units of the last significant figure, is given in parentheses*)

Bond angles		
	O(1)PO(2)	111·0 (1)°
	O(2)PO(3)	107·0 (1)
	O(1)PO(3‴)	111·6 (1)
	O(3)PO(3‴)	108·6 (1)
Interatomic distances		
	P——O(1)	1·540 (2) Å
	P——O(2)	1·544 (2)
	P——O(3)	1·537 (2)*
	O(1)–O(2)	2·542 (3)
	O(1)–O(3)	2·545 (3)*
	O(2)–O(3)	2·476 (3)*
	O(3)–O(3‴)	2·496 (4)
	Sr(1)–O(1)	2·567 (2)**
	Sr(1)–O(2)	2·580 (2)**
	Sr(1)–O(3)	2·859 (2)**
	Sr(2)–O(1)	2·847 (2)
	Sr(2)–O(2)	2·437 (2)
	Sr(2)–O(3)	2·696 (2)*
	Sr(2)–O(3‴)	2·510 (2)*
	Sr(2)–Cl	3·086 (1)
	Sr(2)–Sr(2′)	4·340 (1)

* The number of asterisks indicates the number of times the distance is repeated for symmetry-related sites of the second atom.

† The function and error program of Busing, Johnson, Thiessen & Levy (1973) called *ORFFE*3 was used in the calculations. O(3‴) is related to O(3) by reflection at $z = \frac{1}{4}$. A singly primed symbol designates an atom with coordinates $y-x, -x, z$ and a doubly primed one an atom with coordinates $x-y, x, \frac{1}{2}+z$ where x,y,z are those of the atom designated by an unprimed symbol.

Table 1. *Atomic parameters* (*with estimated standard deviations*)

All values except fractions have been multiplied by 10^4.

	Multiplier	x	y	z	β_{11}	β_{22}	β_{33}	β_{12}	β_{13}	β_{23}
O(1)	5000 (21)	3365 (3)	4821 (3)	$\frac{1}{4}$	43 (3)	35 (3)	58 (4)	32 (2)	0	0
O(2)	5000 (21)	5861 (2)	4662 (3)	$\frac{1}{4}$	18 (2)	24 (2)	101 (5)	7 (2)	0	0
O(3)	10000 (42)	3549 (2)	2670 (2)	768 (2)	68 (2)	40 (2)	57 (3)	35 (2)	−27 (2)	−18 (2)
P	5000 (21)	4052 (1)	3720 (1)	$\frac{1}{4}$	23 (1)	19 (1)	37 (1)	12 (1)	0	0
Sr(1)	3331 (9)	$\frac{1}{3}$	$\frac{2}{3}$	9 (1)	30 (1)	30	9	5	0	0
Sr(2)	5003 (11)	104 (0)	2592 (0)	$\frac{1}{4}$	28 (0)	27 (0)	43 (0)	14 (0)	0	0
Cl	1508 (14)	0	0	$\frac{1}{2}$	30 (2)	30	85 (3)	15	0	0

$z=\frac{3}{4}$. The Sr–Cl distance is 3·086 Å. Sr(2) in the structure has a coordination number 8 (6 oxygen and 2 chlorine ions). Taking the ionic radius of Cl^- as 1·81 Å and that of Sr^{2+} in coordination 8 as 1·25 Å (Shannon & Prewitt, 1969), one sees that the observed Sr–Cl distance is in agreement with the sum of the ionic radii. [In the structure of chlorapatite, 'ClAp', $Ca_5(PO_4)_3Cl$ (Mackie, Elliott & Young, 1972) this site for the Cl atom would result in a Ca–Cl bond distance greater than the sum of the ionic radii. To avoid that, the chlorine atom in ClAp occurs 0·38 Å away from $0,0,\frac{1}{2}$ along the **c** direction].

Comparing this $Sr_5(PO_4)_3Cl$ structure (SrClAp) with that of $Sr_5(PO_4)_3OH$ and various calcium apatites, one sees that the chlorine ions occurring at $0,0,\frac{1}{2}$ (SrClAp) and 0,0,0·444 (ClAp) appear to repel the nearby O(3) ions, thus expanding the entire cell perpendicular to **c**, including the M(2) triangles (see Table 4), where M(2) is either Sr(2) or Ca(2).

The PO_4 groups are similarly but slightly less distorted in the Sr apatites than in the Ca apatites. (In the present structure the phosphate tetrahedra have an average P–O bond length of 1·539 (2) Å, all the four lengths agreeing within two standard deviations, but the same type of regularity is not exhibited in the bond angles.) The PO_4 groups are also rotated away from the higher lattice-symmetry ($P6_3/mcm$) orientation to increasing degree in the order $Ca_5(PO_4)_3Cl$, $Ca_5(PO_4)_3OH$, $Sr_5(PO_4)_3OH$, and $Sr_5(PO_4)_3Cl$.

Table 4. *Comparison of the distances of* O(3) *and* M(2) *from the screw axis for strontium and calcium apatites*

	6_3–O(3)	6_3–M(2)
$Sr_5(PO_4)_3Cl$	3·08 Å	2·51 Å
$Sr_5(PO_4)_3OH$	3·04	2·46
$Ca_5(PO_4)_3Cl$	3·16	2·48
$Ca_5(PO_4)_3OH$	2·90	2·36

Error analysis

In the least-squares refinements, the weights used were reciprocal estimated variances, σ^{-2}, for the individual reflections. Refinements with $\sigma=\sigma_c$, the standard deviation estimated from counting statistics, led to a value greater than 2·5, rather than the expected 1·00,

Table 3. *Squares of observed and calculated structure factors*

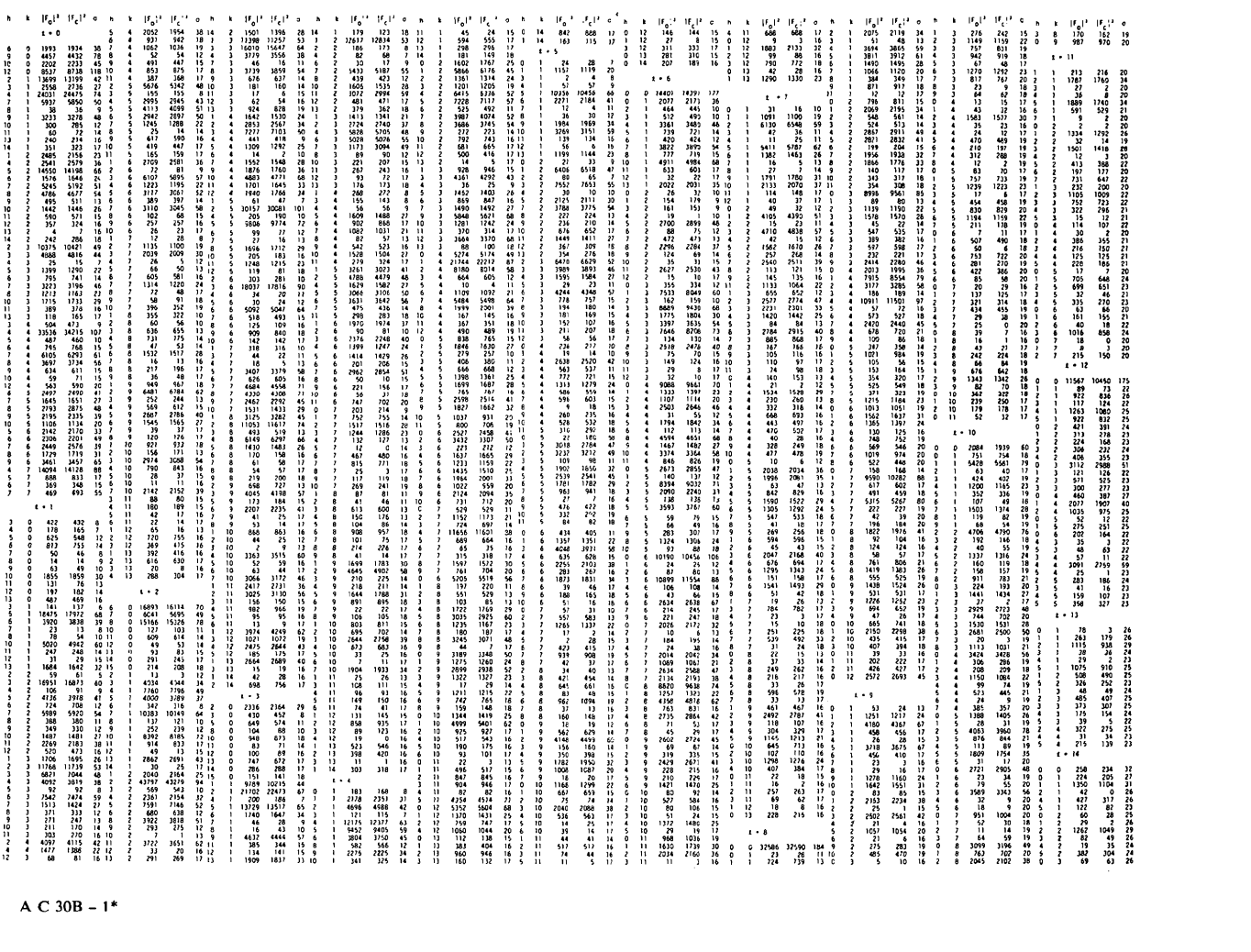

for $\sum_1=\{\sum w(|F_o|^2-|F_c|^2)^2/(m-n)\}^{1/2}$, where m is the total number of observations and n the number of parameters varied. The normal probability plot (δR type; Abrahams & Keve, 1971) was 'S' shaped (Fig. 1) and had a best-straight-line slope of 2·41. The magnitude and source of the additional error, thereby indicated to be present in addition to σ_c, were sought. A strong correlation of the magnitude of an indicated random error with $|F|^2$ was found; the 'envelope' of a $\Delta|F|^2/\sigma$ *vs.* $\log|F|^2$ plot (Fig. 2) showed a horn-shaped character opening toward large $|F|^2$. (Plotting against $\log|F|^2$ rather than $|F|^2$ gave much the more useful display.) A plot of $\Delta|F|^2/\sigma$ *vs.* $\sin\theta/\lambda$ showed an apparent correlation which is probably attributable to the partial correlation of $|F|^2$ with $\sin\theta/\lambda$ (Fig. 3). The estimated variance, σ^2, for each observation was then arbitrarily revised according to

$$\sigma^2=\sigma_c^2+\sigma_x^2$$

where

$$\sigma_x=k|F|^2$$

is the indicated additional random error of unspecified source. Subsequent refinements were carried out with different values assigned for k and the three types of plots described were used to check the distribution of random errors corresponding to each assignment. Setting $\sigma_x=0{\cdot}05|F|^2$ straightened the normal probability plot (Fig. 4) bringing its best-straight-line slope to 1·01 (*vs.* 1·00 ideal) and removed the obvious correlation of $\Delta|F|^2/\sigma$ with $\log|F|^2$ (Fig. 5). (Setting $\sigma_x=0{\cdot}04|F|^2$ resulted in 1·13 for the slope in the normal probability plot; $\sigma_x=0{\cdot}06|F|^2$ resulted in a slope of 0·93.)

As is algebraically evident from the variance expression that worked well ($\sigma^2=\sigma_c^2+\sigma_x^2$), the horn-shaped

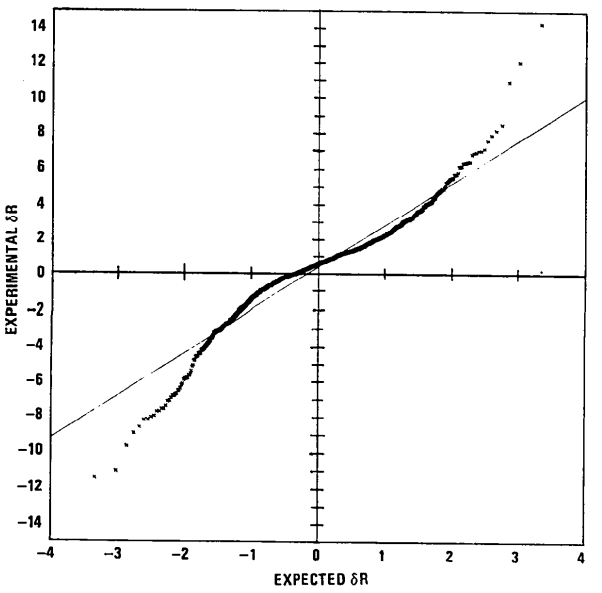

Fig. 1. Normal probability plot for δR with $\sigma=\sigma_c$. The slope of the best straight line is 2·41.

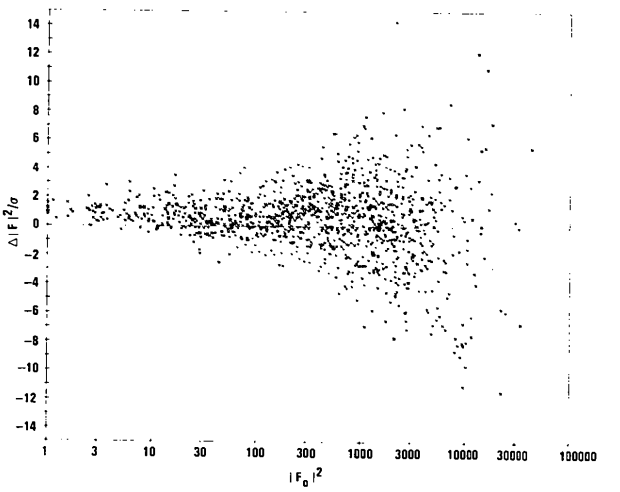

Fig. 2. Semi-log plot showing the correlation of $\Delta|F|^2/\sigma$ with $|F|^2$ for $\sigma=\sigma_c$.

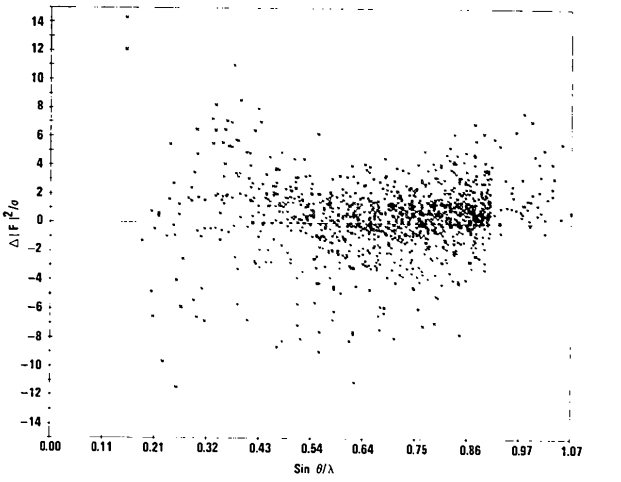

Fig. 3. Plot showing the partial correlation of $\Delta|F|^2/\sigma$ with $(\sin\theta)/\lambda$ for $\sigma=\sigma_c$.

character in $\Delta|F|^2/\sigma$ *vs.* $\log|F|^2$ should be confined to the range of $|F|^2$ where dominance is shifting from the σ_c term to the σ_x term. As would therefore be expected, in a refinement with data from a spheroidal crystal of fluorapatite (Mackie, 1972) for which $\sigma_c\leq 1\%|F|^2$ for nearly all reflections, the horn-shaped character was not evident except, possibly, in the lower range of $|F|^2$.

The failure of the normal probability plot to pass through the origin is not uncommon [see for example Abrahams & Keve (1971), Fig. 7], even though the overall scale factor has been adjusted along with the other parameters in the full-matrix least-squares refinement. This failure reflects a difference between the median (on which the origin of the plot is based) and the arithmetic mean (on which the scale factor is based) of the $\Delta|F|^2$ values, something that would not be possible for a normal distribution except for the fact that the arithmetic mean used here is actually a

weighted mean. The fact that the median is higher than the mean is also indicated in Fig. 5 by the appearance of more positive than negative values of $\Delta|F|^2/\sigma$. Production of this effect requires that the reflections for which $\Delta|F|^2$ is negative must be weighted more heavily (have smaller σ values) on the average than are those for which $\Delta|F|^2$ is positive. The appearance of a general slightly negative slope in the aggregate of points in Fig. 5 suggests that this is what has occurred in the present data set, as there appears to be a slight correlation of negative $\Delta|F|^2$ with the large $|F|^2$. That, in turn, suggests that the uncertainties in the strong reflections are still underestimated even though $\sigma_x=0{\cdot}05|F|^2$ has been included.

Possible sources of σ_x to be considered include instrument instability, absorption correction errors, model inadequacies, counter dead-time counting losses, extinction errors, and crystal inhomogeneity with respect to diffraction, perhaps among others. Instrument instability was shown by several tests to be less than 1%, *e.g.* two independent collections of 231 reflection-intensity data from the same fluorapatite crystal (Mackie, 1972) yielded a mutual R index of 0·67%; thus, only a small portion of σ_x should be attributed to instrument instability. In Mackie's (1972) refinement with the spheroidal crystal $\sum_1=3{\cdot}53$ and the indicated σ_x was, again a few percent of $|F|^2$. It would seem unlikely that the pseudo-randomly distributed absorption-correction errors would be nearly as large for that spheroidal specimen as for the present crystal of natural shape. Thus, absorption correction errors do not appear to be a probable source of the bulk of σ_x. The fact that the 'horn' in the $\Delta|F|^2/\sigma$ *vs.* log $|F|^2$ opened toward large $|F|^2$ indicates that σ_x is not primarily due to model inadequacies. It seems that uncorrected extinction cannot be the source of σ_x because (i) the extinction corrections were carried through to completion as a part of the least-squares refinement, (ii) inspection of the structure factor tables showed no characteristic excess of $|F_c|^2$ over $|F_o|^2$ for strong reflections, and (iii) the extinction correction was generally very small (~25%, ~6%, and ~4% in 2 cases each, less than 2% in the other 1168 cases). Counting losses due to counter dead-time seem not to be a significant contributor to σ_x, as (i) the intensity at no time reached that at which attenuators were programmatically inserted into the beam and (ii) test data covering both strong and weak reflections gave the same results for relative intensities both with and without attenuators in the beam. The possibility remains that it may be due to a variety of crystal imperfections (Hamilton, 1972), *i.e.* crystal inhomogeneity with respect to diffraction.

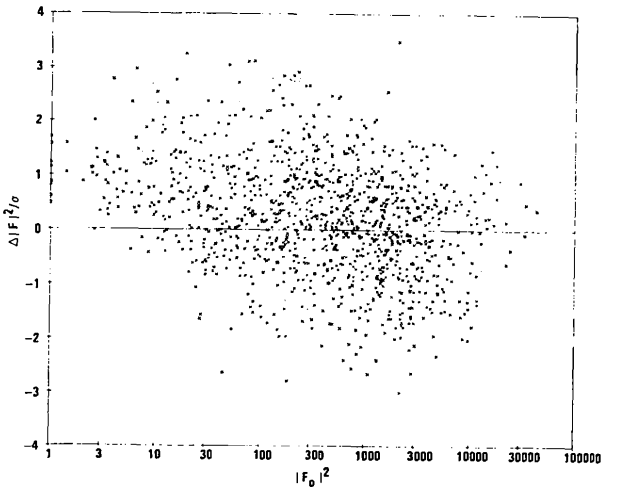

Fig. 5. Semi-log plot of $\Delta|F|^2/\sigma$ *vs.* $|F|^2$ with $\sigma^2=\sigma_c^2+(0{\cdot}05|F|^2)^2$.

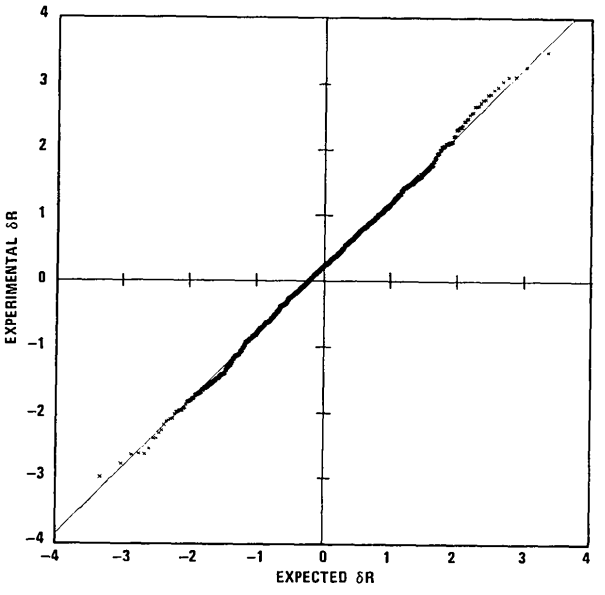

Fig. 4. Normal probability plot for δR with $\sigma^2=\sigma_c^2+(0{\cdot}05|F|^2)^2$. The slope of the best straight line is 1·01.

The occurrence of a random error representable by a σ_x corresponding to a few percent is, apparently, not uncommon. In all of the several tens of structure refinements of apatites done in this laboratory in recent years the value of $\sum_1$ obtained suggests the existence of such a σ_x term. Other workers have also found consistent need for the inclusion of such a term (Hamilton, 1972; Verbist, Lehmann, Koetzle & Hamilton, 1972; Coppens, 1972). Mais, Owston & Wood (1972), in particularly careful assessment of errors in refinements of K_2PtCl_4 and K_2PdCl_4, found an unexplained uncertainty in the structure amplitudes of approximately 2% (which is comparable to 4% in $|F|^2$ used here). As they note, 'the next step in improving accuracy evidently must be to find reasons for this, at present unexplained, variation'.

Inclusion of the σ_x term required to straighten the normal probability plot and to remove the correlation of $\Delta|F|^2/\sigma$ with log $|F|^2$ and to make $\sum_1\approx 1$ increased wR_2 from 4·4 to 7·1%, yet only one of the 42 param-

eters was changed by as much as $2\sigma_p$ ($\sigma_p < 5\%$ for thermal parameters and $\sigma_p < 0{\cdot}0003$ for positional parameters) where σ_p is the error calculated for parameters varied in refinement before the σ_x question was taken up. Therefore, while the source of the additional random error σ_x has not been identified, and could be especially interesting, there is as yet no evidence that ignoring σ_x produces significant parameter errors in a structure refinement that is otherwise well done.

We thank Dr N. M. Braun, General Electric Company, Cleveland, for the chemical analyses of the strontium chlorapatite crystal-growth batch and the U.S. Public Health Service for financial support through NIH-NIDR Grant DE 01912.

References

ABRAHAMS, S. C. & KEVE, E. T. (1971). *Acta Cryst.* A**27**, 157–164.
BUSING, W. R., JOHNSON, C. K., THIESSEN, W. E. & LEVY, H. A. (1973). *ORFFE*3. Accession No. 85, World List of Crystallographic Computer Programs, 3rd ed., *J. Appl. Cryst.* **6**, 309–346.
BUSING, W. R. & LEVY, H. A. (1957). *Acta Cryst.* **10**, 180–182 (*ORABS*-2 by H. A. LEVY & R. D. ELLISON was used).
BUSING, W. R., MARTIN, K. O. & LEVY, H. A. (1962). *ORFLS*. Report ORNL-TM-305, Oak Ridge National Laboratory, Oak Ridge, Tennessee.
COLLIN, R. L. (1959). *J. Amer. Chem. Soc.* **81**, 5275–5278.
COPPENS, P. (1972). Private communication.
CROMER, D. T. (1965). *Acta Cryst.* **18**, 17–23.
CROMER, D. T. & WABER, J. T. (1965). *Acta Cryst.* **18**, 104–109.
CURZON, M. E. J., ADKINS, B. L., BIBBY, B. G. & LOSEE, F. L. (1970). *J. Dent. Res.* **49**, 526–528.
ELLIOT, J. C., MACKIE, P. E. & YOUNG, R. A. (1973). *Science*, **180**, 1055–1057.
ELLISON, R. D., HAMILTON, W. C., IBERS, J. A., JOHNSON, C. K. & THIESSEN, W. E. (1971). *ORXFLS*3.
HAMILTON, W. C. (1972). Private communication.
MACKIE, P. E. (1972). Ph. D. Thesis, Georgia Institute of Technology, Atlanta, Georgia 30332, U.S.A.
MACKIE, P. E., ELLIOT, J. C. & YOUNG, R. A. (1972). *Acta Cryst.* B**28**, 1840–1848.
MAIS, R. H. B., OWSTON, P. G. & WOOD, A. M. (1972). *Acta Cryst.* B**28**, 393–399.
NÁRAY-SZABÓ, ST. (1930). *Z. Kristallogr.* **75**, 387–398.
SHANNON, R. D. & PREWITT, C. T. (1969). *Acta Cryst.* B**25**, 925–946.
SUDARSANAN, K., MACKIE, P. E. & YOUNG, R. A. (1972). *Mater. Res. Bull.* **7**, 1331–1338.
SUDARSANAN, K. & YOUNG, R. A. (1969). *Acta Cryst.* B**25**, 1534–1543.
SUDARSANAN, K. & YOUNG, R. A. (1972). *Acta Cryst.* B**28**, 3668–3670.
SUDARSANAN, K., YOUNG, R. A. & DONNAY, J. D. H. (1973). *Acta Cryst.* B**29**, 808–814.
TOKONAMI, M. (1965). *Acta Cryst.* **19**, 486.
VERBIST, J. J., LEHMAN, M. S., KOETZLE, T. F. & HAMILTON, W. C. (1972). *Acta Cryst.* B**28**, 3006–3013.

Acta Cryst. (1974). B**30**, 1386

Structure Cristalline et Moléculaire de la Phellibiline: Alcaloïde du Groupe de l'Homoérythroïdine

PAR CLAUDE RICHE

Laboratoire de Cristallochimie, Institut de Chimie des Substances Naturelles du CNRS, 91190-Gif/Yvette, France

(*Reçu le* 17 *décembre* 1973, *accepté le* 17 *janvier* 1974)

The alkaloid phellibiline, $C_{16}H_{21}NO_3$, is the first member of the homoerythroidine group. It crystallizes in the monoclinic space group $P2_1$ with $a = 8{\cdot}681$, $b = 9{\cdot}365$, $c = 8{\cdot}684$ Å, $\beta = 97{\cdot}8°$, $Z = 2$. The structure has been determined by direct methods from data collected with Cu $K\alpha$ radiation on Weissenberg photographs, and refined by least-squares methods to a final R value of 0·09 for 1395 observed reflexions. The X-ray analysis confirmed the planar formula and established the configuration of the molecule.

Introduction

L'étude chimique des constituants de *Phelline billiardieri* (Ilicacées) a permis d'isoler les premiers alcaloïdes du groupe de l'homoérythroïdine. Les formules planes (I) et (II) ont été proposées pour la phellibiline, la formule (I) étant considérée comme la plus probable d'après l'analyse des spectres de résonance magnétique nucléaire (Nhu Mai, Langlois, Das & Potier, 1970).

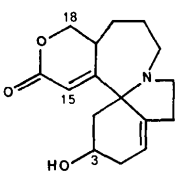

(I)

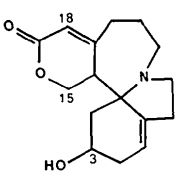

(II)

La détermination de la structure cristalline de la phellibiline a été entreprise pour établir avec certitude la formule plane et pour en définir la stéréochimie.